Fatigue Failure Assessment Considering Actual-Working Load and Running Position of Orthotropic Steel Deck by using BWIM

Yoshihiko TAKADA*, Takashi YAMAGUCHI**

(Received September 8, 2009)

Synopsis

Recent considerable increases in traffic intensity and wheel loads are causing fatigue cracks in orthotropic steel decks in Hanshin Expressway .From results of the periodic inspection, fatigue cracks are detected by 167 spans in 1347 spans in orthotropic steel decks as of April, 2009. Under traffic loading, in particular the effect of local wheel loads, longitudinal welds between deck plate and trough are subjected to local transverse bending moments and are susceptible to fatigue cracks. The stress in trough to deck plate welds is strongly influenced by actual-working load and run position .Then, in orthotropic steel decks in Kobe route of Hanshin Expressway, measurement of the load of actual-working traffic and generating stress is performed by Bridge-Weigh-In-Motion. This papert presents the outline of fatigue failure in orthotropic steel decks. Next, Fatigue failure assessment based on this measurement results are described

KEYWORDS: Orthotropic Steel Deck, Bwim(Bridge-Weigh-In-Motion), Fatigue Failure Assessment Actual-Working Traffic Load, Run Position

1. Introduction

Hanshin Expressway Public Corporation has been constructing and operating an urban expressway network in Kansai Metropolitan Area for over 45 years. The network currently expands to 233.8 km in total length and is used averagely by about 890,000 vehicles. About 90% of Hanshin Expressway (HEW) consists of viaduct structures. Among 6,500 spans of bridges, 1,347 are orthotropic steel decks (OSD). Although all the longitudinal stiffener in OSD was composed by bulb rib in the completion before 1980, trough have been adopted since then.

Recent considerable increases in traffic intensity and wheel loads are causing fatigue cracks in OSD. From results of the periodic inspection, fatigue cracks are detected by the 167 spans in OSD of April 2009. Under traffic loading, in particular the effect of local wheel loads, longitudinal welds between deck plate and trough are subjected to local transverse bending moments and are susceptible to fatigue cracks. The stress in trough to deck plate welds is strongly influenced by actual-working load and run position. Then, in OSD in Kobe route, measurement of the load of actual-working traffic and generating stress is performed by Bridge-Weigh-In-Motion (BWIM).

2. Overview of the current traffic in HEW

HEW network in the Kansai Metropolitan Area linking the major cities of Osaka, Kobe and Kyoto currently expands to 233.8 km in total length and is used averagely by about 890,000 vehicles. The large vehicles ratio of HEW are approximately 20% on the average as a result of the origin-destination survey. The daily traffic volume is 50,000 vehicles per two lanes in the routes within urban, and 40,000 vehicles per 2 lanes in Wangan Route. In those routes, large vehicles ratio is high with an average of 30%[1].

Axle load measuring device is installed in all the tollgates in order to find the violation vehicles of axle loads. Figure 1 shows the mixing rate of weight of vehicles and the mixing rate of axle loads in the main intensive tollgates. Weight of vehicle is regulated by law by 245kN or less[2]. Axle load is also regulated by 89kN or less. Nakazima tollgate located in Wangan-Route and Ashiya tollgate located in Kobe-Route have many violation vehicles. In Ashiya tollgate, 32% of trailers are violation of vehicle weight, 19% are violation of axle load.

3. The overview of the inspection of OSD of HEW

The facility quantity of OSD are 1347 spans shown in Table 1. The specification of them are 714 spans of trough, and 633 spans of bulb rib. Almost all the OSD constructed before 1980 were the structures which used the bulb rib. After it, the trough has adopted .

Superstructures, such as OSD, are performing the periodic inspection for all the routes by approach viewing with the cycle of 4 to 8 years. The typical fatigue cracks in troughs are shown in Figure 2. Such fatigue cracks are

* Student, Doctor Course of Dept. of Civil Engineering

** Professor, Department of Civil Engineering

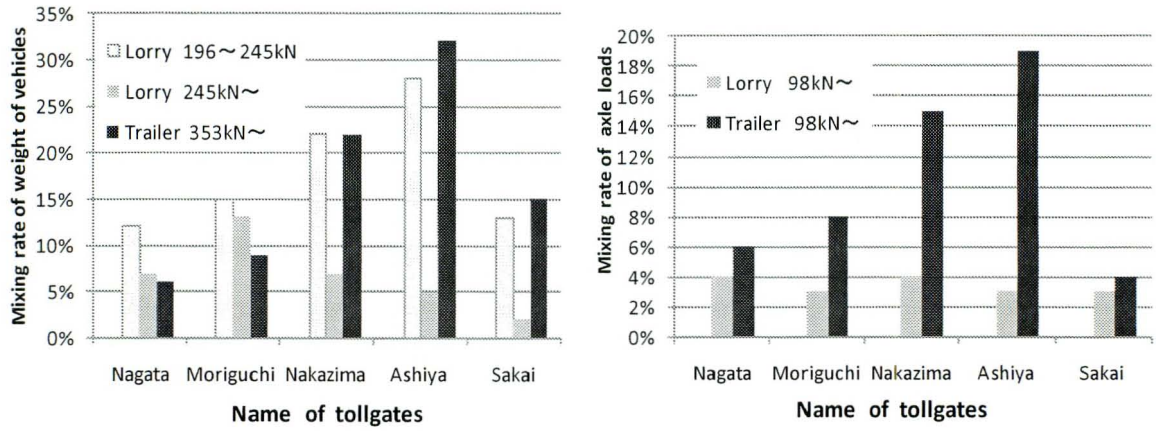

Fig. 1 Violation vehicle weight and axle load

classified according to the structure of the longitudinal rib of OSD. The deck plate is taken as 12 mm, for most bridges the common plate thickness in combination with the asphalt layer with the thickness of 80mm. Trough web thickness is 6 mm[3].

Table 2 gives crack classified into crack type. The overview of five types of cracks which exist in trough form are as follows. Penetrating cracks in deck plate (type-s) was detected by Shinhamadera Bridge located in Wangan Route in 2005. This crack type may a threat of traffic safety if the crack progresses considerably. Petrating cracks in weld bead (type-1) exist in 137 cracks on the bridges of 23 spans. Cracks in trough longitudinal stiffeners splice joint (type-2) exist in 60 cracks. Crack in weld between vertical stiffener and deck plate (type-3) is detected in 256 cracks. This type of crack have the examples penetrated to the deck plate, and may conduct damage to pavement. As for crack in connection between trough profiles and crossbeam (type-4), 261 cracks are detected by 34 spans.

Table 1 Classification of rib form in OSD

	Spans	Extension (Km)
Bulb rib	718	40.99
Trough	629	43.35
Total	1347	84.34

Table 2 Crack classification

	Crack	Spans	Cracks
Type-s	Penetrating crack in deck plate	1	2
Type-1	Petrating crack in weld bead	23	137
Type-2	Crack in trough longitudinal stiffeners splice joint	21	60
Type-3	Crack in weld between vertical stiffener and deck plate	43	256
Type-4	Crack in connection between trough profiles and crossbeam	34	261
	Others	5	155
	Total	127	731

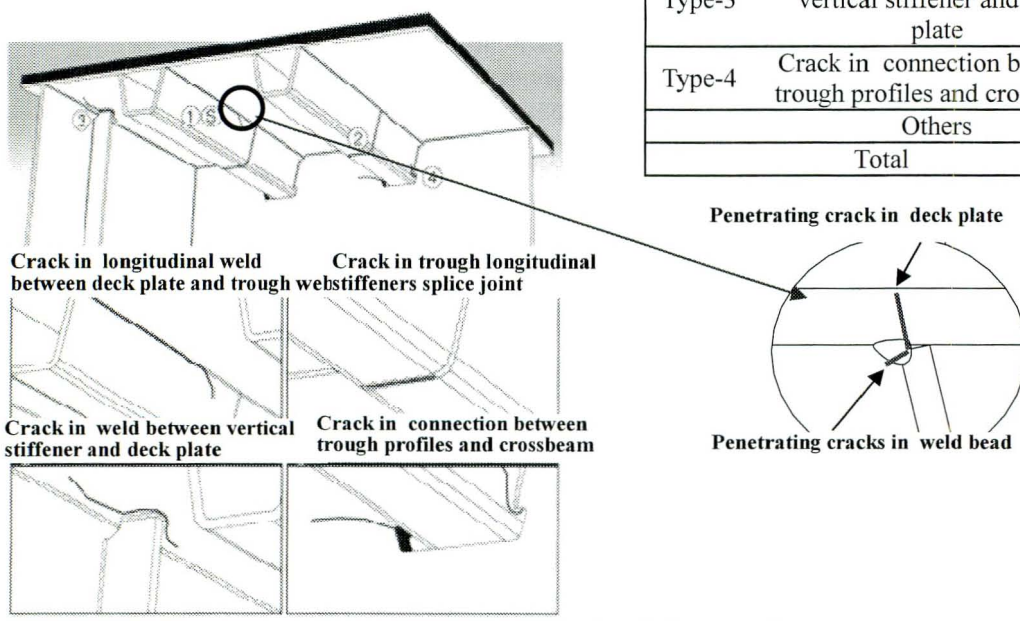

Fig. 2 Typical fatigue cracks

4. Fatigue cracks phenomenon in trough

4.1 Penetrating cracks of deck plate

Penetrating crack of deck plate was detected by Shinhamadera Bridge located in Wangan Route in 2005[4]. Figure 3 shows the crack on a deck plate. This bridge was opened in 1993. This crack was detected by chance when asphalt paving was removed. The 6 mm thick trough were butt-welded to 12 mm thick deck plates. The total thickness of a two-layer pavement is 65 mm. Water spilled from trough rib below the fatigue crack during inspection. A detailed inspection was carried out from the deck top using MT. The length of the crack was 520 mm, which is longer than the 450 mm observed visually. The crack disappeared after grinding down 3 mm in depth at a crack tip, as shown in Figure 4(a). The fracture surface showed evidence of friction of the surfaces either side of the crack in the intermediate part of the crack in Figure 4(b). Crack bifurcation (branching) was clearly observable at another crack tip in Figure 4(c)

Two vertical holes were cut into the deck plate at both crack tips to restrict crack growth and to inspect. MT, applied for detection of inside defects at the drilled cores, also indicated that the crack propagated from the interior rib-to-deck weld to the deck surface while changing direction, as shown in Figure 5. Macro-fractographic observations showed the 6mm longitudinal ribs had 2 mm penetration welds, which were about 30 percent penetration, as shown in Figure 6. In order to prevent growth of the crack and to ensure the safety of traffic, an emergency repair with splice-plates has carried out.

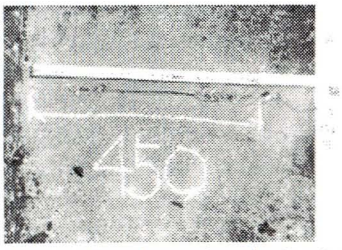

Fig. 3 Crack on the deck plate

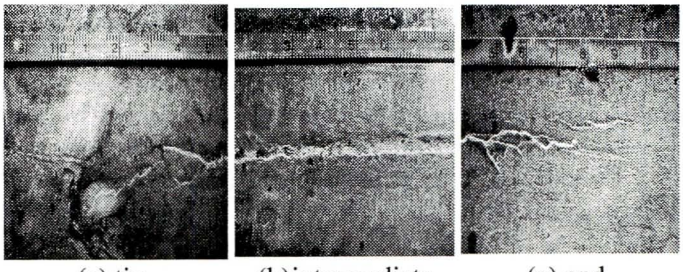

(a) tip (b)intermediate (c) end

Fig. 4 Magnetic Particle Testing

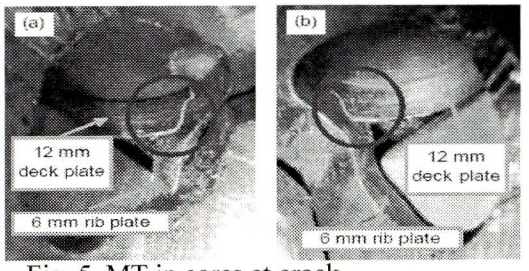

Fig. 5 MT in cores at crack

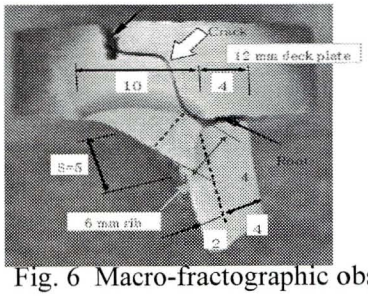

Fig. 6 Macro-fractographic observation

4.2 Penetrating crack in weld bead

Penetrating crack in weld bead is shown in Figure 7. This crack initiation is at weld root inside the trough. In the initial phase, growth of the crack is the thickness direction of the fillet weld. The crack which penetrated the throat depth appears to grow up along the root of the longitudinal fillet weld. In this phase, the cracks had a example which grew 10mm per week. Finally, this crack type may grow up to trough profiles and deck plates. 66 cracks in this type of all the cracks (137 cracks) had grown to be the trough profiles. In the branch point of the crack, the remains of the piece for erection existed in the deck plate upper surface. Figure 8 shows frequency of length to all the cracks in the longitudinal weld between deck plate and trough webs. The length of the average of these cracks is 458mm.

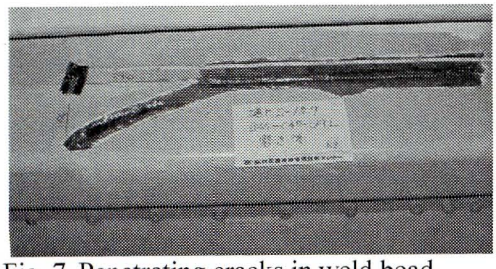

Fig. 7 Penetrating cracks in weld bead

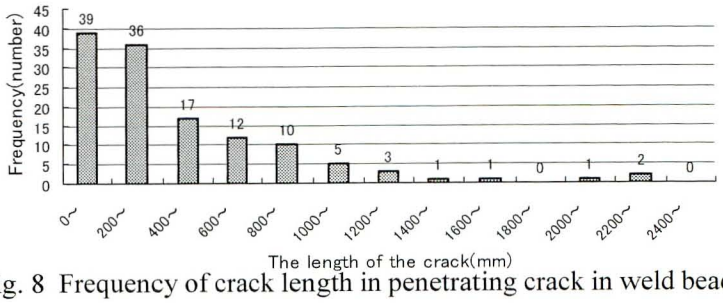

Fig. 8 Frequency of crack length in penetrating crack in weld bead

5. Actual-working load and run position on OSD applied in BWIM

Under traffic loading, in particular the effect of local wheel loads, longitudinal welds between deck plate and trough are subjected to local transverse bending moments and are susceptible to fatigue cracks. The stress in trough to deck plate welds is strongly influenced by actual-working load and run position. Then, in OSD in Kobe route, measurement of the load of actual-working traffic and generating stress is performed by BWIM[5].

5.1 The measured bridge

The measured bridge is a simple orthotropic-steel-deck plate girder bridge of trough form, as shown in Figure 9. This bridge was reconstructed after Kobe Earthquake and has started the open to traffic in August, 1997. The bead penetration crack was detected in the weld between deck plate and trough web in December, 2002, and the emergency retrofit was performed by site welding in 2005. Then, the periodical inspection has performed and the crack is not detected in the present.

Measurement of actual working traffic is performed by the reaction force method which is the typical method of BWIM. Stress measurement of OSD also performed. The run position of the axle is measured by a laser range meter located at the road shoulder of an emergency parking bay. BWIM is calibrated by comparison with the generating stress of the inspection car of 245kN.

A reaction force method is the method of BWIM of searching for axle loads using the strain response waveshape on the support generated by passage of an axle as shown in Figure 10. The strain are measured by strain gauges pasted on the vertical stiffener on support. Concretely, axle loads are calculated by the rapid difference of the strain on support in both entrance and recession of vehicles. Besides, velocity of run vehicles is calculated from the difference of generating time of these strains and span length. The result of analysis of these strains leads the traffic according to type of cars, passage velocity, axle loads, gross weights, etc. In load evaluation, it is necessary to calculate for the frequency of a vehicles load and an axle load for every typical type of cars. Then, the classification of the type of a car of run vehicles is presumed by the analysis of the number of axes of vehicles, the distance of an axle, and an axial arrangement pattern.

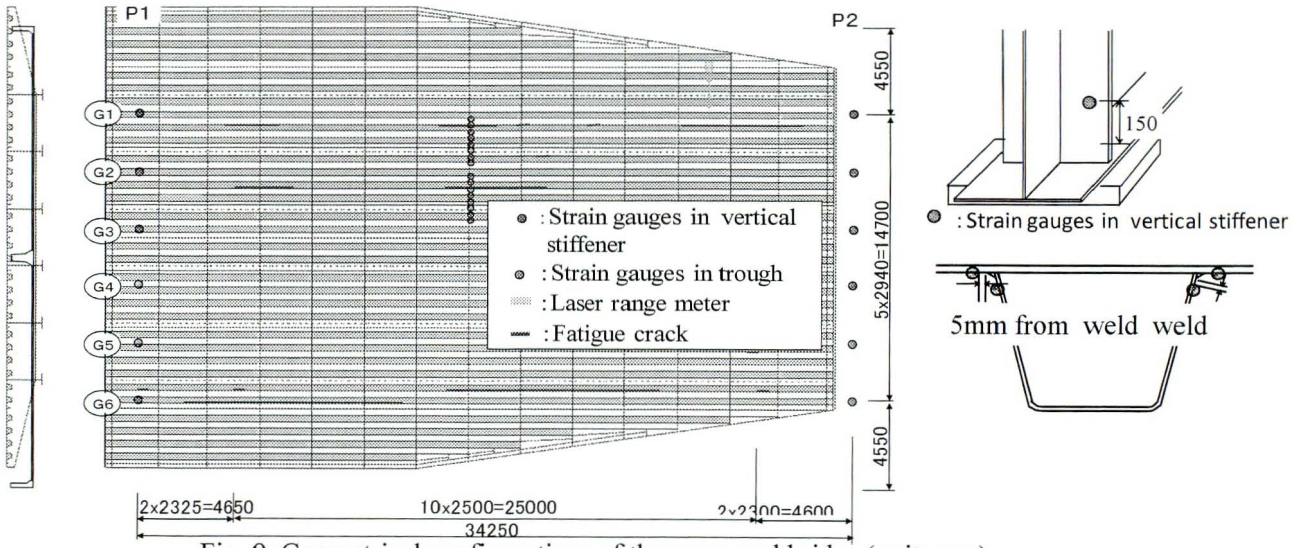

Fig. 9 Geometrical configurations of the measured bridge (unit: mm)

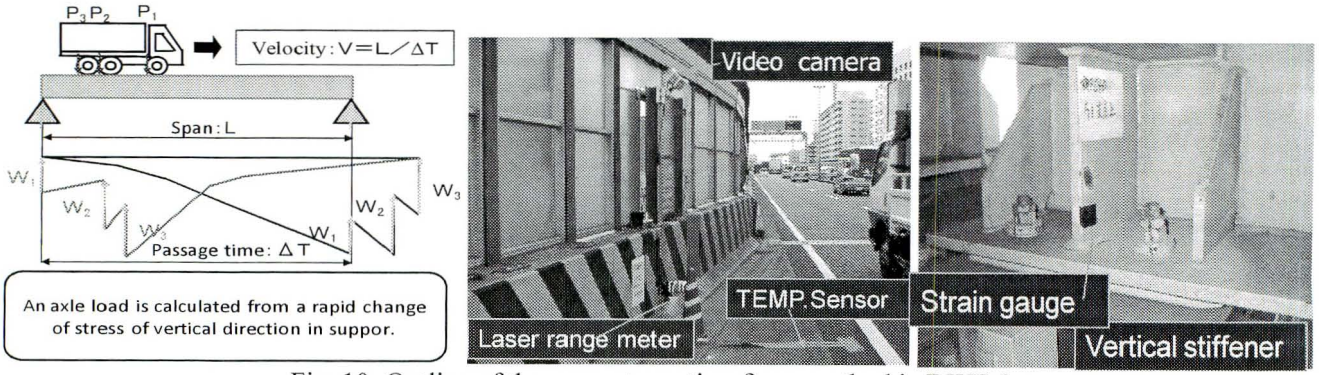

Fig. 10 Outline of the support reaction-force method in BWIM

5.2 Weight of vehicle and axle load distribution

Table 3 is the analysis result of weight of vehicle and axle load by the classification of the type of cars. Traffic volume measured by BWIM are 17, 159 cars in the fast lane and 11, 671 cars in the slow lane in total for three days. The passenger car is not included in these numbers. The maximum weight of vehicle in the slow lane is 23.7tf in small size and medium size car, 395.9kN in track ,and, 707.6kN in trailer. The maximum axle load is 174.4kN in small and medium size car, 169.5kN in track, and, 197kN in trailer. The slow lane shares 61% of number of tracks and 62% of number of trailers to all the lanes. The numbers of average axes for every type of cars are 3.2 axes in tracks and 3.2 axes in trailers. Since the difference of the traffic volume by lane is large, in evaluation of fatigue, measurable BWIM directly per lane is the fine method.

Figure 11 shows frequency analysis of weight of vehicle and axle load in the slow lane. In weight of vehicle distribution, the peaks are in 78kN and 157kN, and average is 176kN. In axle load distribution, the axle load of a peak and average is mostly in agreement, and it is 59kN. Axes exceeding 980kN of legal axle load is 8% of the whole.

Table 3 Summary of vehicle classification

		weight of vehicle			Axle load		
		small and medium size car	Lorry	Trailer	small and medium size car	Lorry	Trailer
Slow lane	Maximum (kN)	232.3	395.9	707.6	174.4	169.5	197.0
	Minimum (kN)	50.0	89.2	110.7	19.6	23.5	25.5
	Average (kN)	94.1	200.9	332.2	47.0	61.7	77.4
	Standard deviation	29.4	48.0	119.6	19.6	20.6	26.5
	Date (cars/axles)	6720	8030	2409	13438	25956	10346
	Dotal (cars/axles)	17,159			49,740		
Fast lane	Maximum (kN)	214.6	331.2	567.4	160.7	145.0	173.5
	Minimum (kN)	50.0	81.3	93.1	19.6	20.6	20.6
	Average (kN)	83.3	168.6	242.1	42.1	52.9	55.9
	Standard deviation	25.5	45.1	80.4	16.7	17.6	19.6
	Date (cars/axles)	4933	5311	1427	9866	16831	6212
	Dotal (cars/axles)	11,671			32,909		

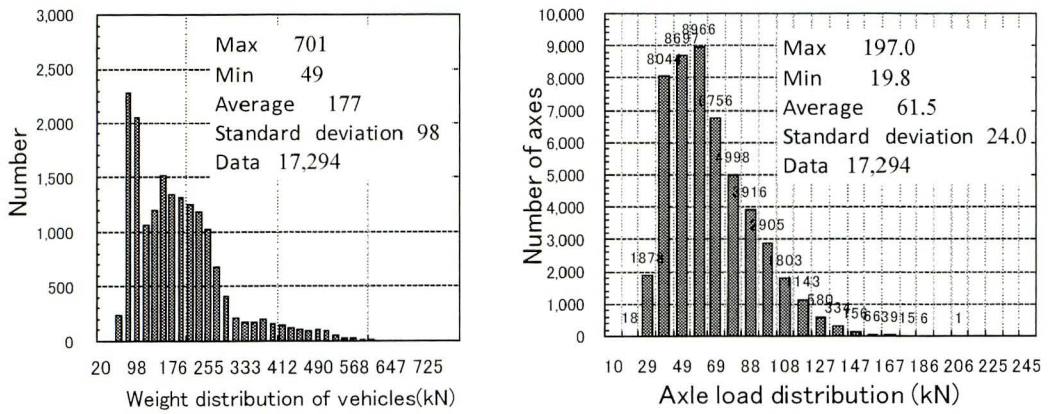

(a)Weight distribution of vehicles (b) Axle load distribution

Fig. 11 Weight distribution of vehicles and axle load distribution in the driving lane (72-hour measurement)

5.3 Vehicle run position

A vehicles run position is measured using a laser range meter. The laser range meter installed in the road shoulder measures the distance to the left tire location of passing cars. The measurement result took the synchronization to measurement of the axle load by BWIM. Frequency distribution of the vehicles run position according to type of cars is shown in Figure 12. This figure shows the run position of the tire from lane space marks. Averages and standard deviation of the vehicles run position according to type of cars are μ=626 mm and σ=226 in small size and medium size cars, μ=627mm σ=179mm in track, and μ=590mm, σ=165mm. Standard deviation of trailers is smaller than that of tracks because the width of vehicles is small. In previous study, run position distribution is σ=300～400mm in large-sized vehicle and σ=400-500 mm in all the types of cars, in case of running the highway. The run position distribution measured this time is smaller than they. This reasonr is because the width of road shoulder in highway with 1.75m is narrower than that of measurement spot with 1.15m.

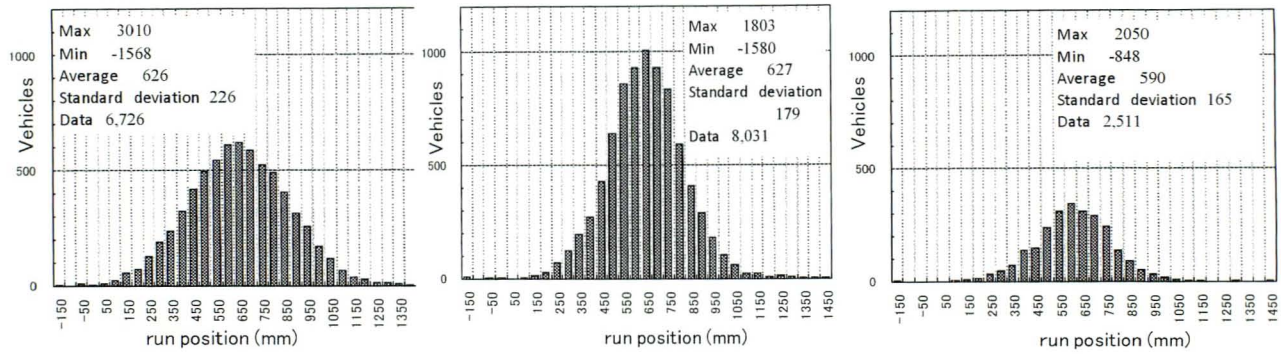

a)Small and medium-size car b)Lorry c)Trailer

(a) Run distribution of left tires

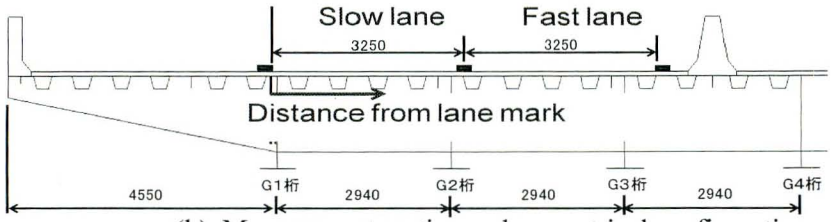

(b) Measurement section and geometrical configurations

Fig. 12 Run distribution of left tires

5.4 Calculation of an equivalent axle load

Axle load distribution is analyzed by the target in the run position location to type of cars. Figure 13 is axle load distribution in the run position of left tire in the slow lane of Figure 12. The run position of large sized vehicles with the axle load exceeding 980 kN is mainly 200-800mm from lane space marks. The run position of the maximum frequency at this time is 600mm.

Next, the equivalent axle load: Weq is calculated based on the axle load measurement data of large-size cars. The equivalent axle load is computed from Eq. (1) of an equivalent average of the 3rd square based on axle load frequency distribution of the vehicles shown in Figure 12.

$$W_{eq} = \sqrt[m]{\sum W_i^{\,m} \cdot n_i / \sum n_i} \qquad (1)$$

Where *Weq* is an equivalent axle load (kN), *Wi* is measurement axle load, *ni* is number of axes, and, *m* is grade of a fatigue design curve :m=3

Figure 14 is frequency distribution of run position and the equivalent axle load according to run position are put. The equivalent axle load of the large-size car in the slow lane is 81.3kN. However, an equivalent axle load with a run position of 200-800mm is 81.3 - 87.2kN (average 85.2kN). An equivalent axle load does not have a great difference by run position. The equivalent axle loads of the run position over 800mm are 68.6kN smaller than 72.5kN of average. Most of vehicles of this area are small and medium size cars.

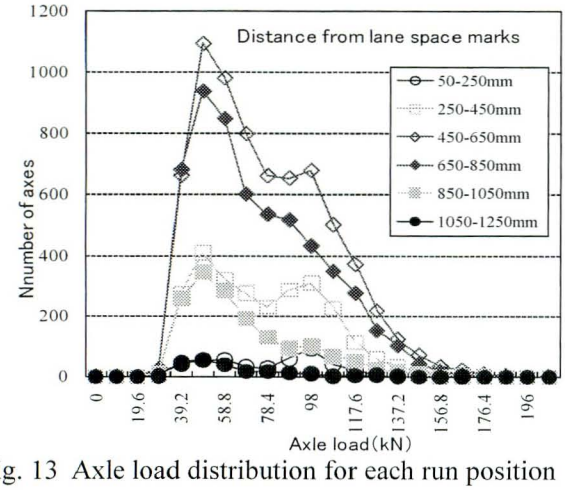

Fig. 13 Axle load distribution for each run position

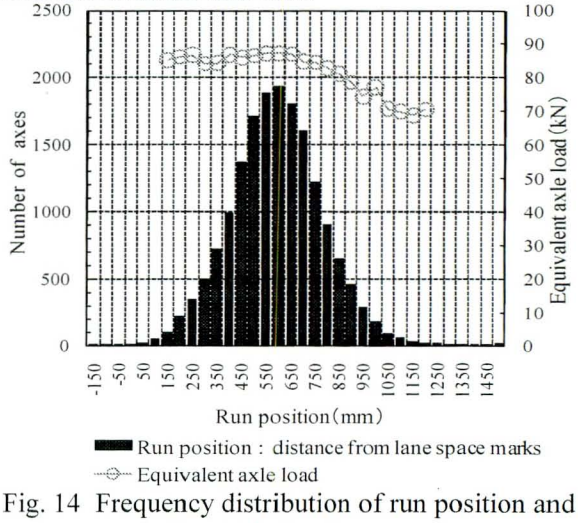

Fig. 14 Frequency distribution of run position and the equivalent axle load

5.5 Relation between tire location and stress range

In order to clarify relation between run position of transverse direction and generating stress, the test car ran at a low speed, making it move to transverse direction every 50mm. The run position is measured for every front axis and back axis using a laser range meter. The stress range of weld toe by trough are computed to the run position. As the result, relation between tire location and stress range is shown in Figure 10. From the approximated curve of stress range, stress range fall to a half in the location distant from the weld of trough and deck plate about 600mm. The generating stress by vehicles run is influenced by run position in addition to the magnitude of an axle load.

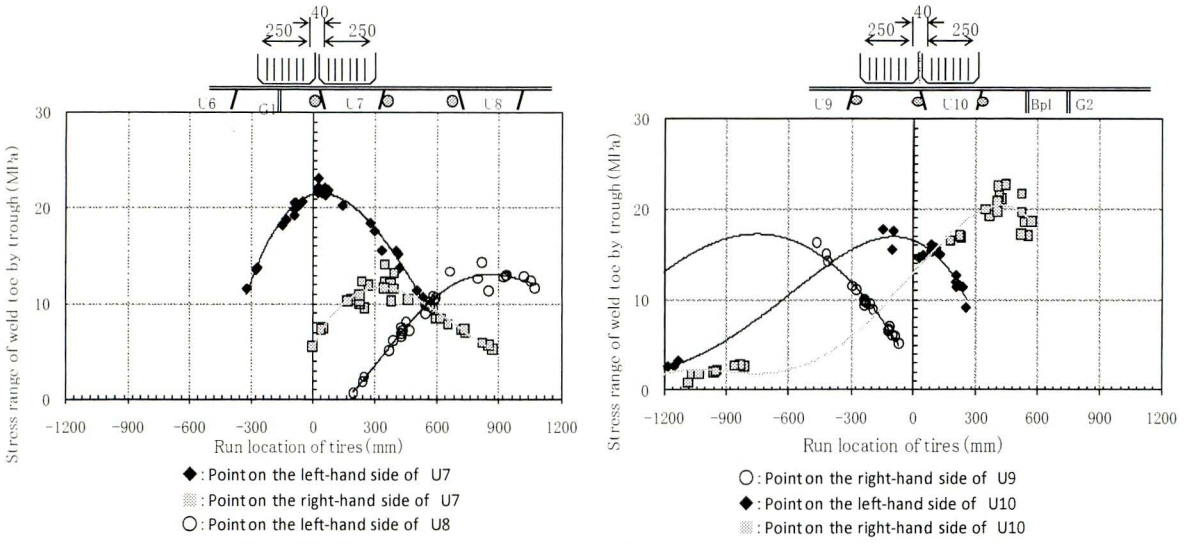

Fig. 15 Relation between tire position and stress range

6. Concluding remarks

The result of fatigue failure assessment of actual-working load and run position of orthotropic steel deck applied in BWIM, followings are concluded

(1)Fatigue cracks are detected by 127 spans of 629 spans in troughs of orthotropic steel decks from results of the periodic inspection in HEW as of March, 2009.

(2)The result of measurement by Axle load measuring device, in Ashiya tollgate, 32% of trailers are violation of vehicle weight, 19% are violation of axle load.

(3)In weight of vehicle distribution by BWIM, the peaks are in 78kN and 157kN, and average is 176kN. In axle load distribution, the axle load of a peak and average is mostly in agreement, and it is 59kN. Axes exceeding 980kN of legal axle load is 8% of the whole.

(4)Averages and standard deviation of the vehicles run position according to type of cars are μ=626 mm and σ=226 in small size and medium size cars, μ=627mm σ=179mm in track, and μ=590mm, σ=165mm.

(5)The equivalent axle load of the large-size car in the slow lane is 81.3kN.

(6)From relation between tire location and stress range, stress range fall to a half in the location distant from the weld of trough and deck plate about 600mm. The generating stress by vehicles run is influenced by run position in addition to the magnitude of an axle load.

7. References

1)Road Structure Ordinance, Japan Road Association, 2006 (in Japanese).

2)Yoshihiko Takada, Yashumito Aoki and Masahiro Sakano, Examination and review of fatigue cracks in orthotropic steel decks in Hanshin Expressway, *Proceedings of 7th German-Japanese Bridge Symposium*, 2007.

3) Hanshin Expressway Public Corporation, Steel Bridge Design Standards, 1985 (in Japanese).

4)Sugioka1.K, Tabata.A, Takada.Y, and Yamamura.K, Investigation and reinforcement for fatigue crack damages on an orthotropic steel deck bridge, *Proceedings of Pacific Structural Steel Conference 2007*, New Zealand, 2007.

5)Yoshihiko Takada, Minoru Kishiro, Takashi Nakashima, Kimihisa Usui, Fatigue failure assessment of actual-working load and run location on orthotropic steel deck applied in BWIM, *Journal of Structure Engineering*, JECE, Vol. 55A, pp. 1456-1467, 2009 (in Japanese).